

NOVEL RADAR SIGNAL MODELS USING NONLINEAR FREQUENCY MODULATION

Sebastian Alphonse and Geoffrey A. Williamson

Department of Electrical and Computer Engineering,
Illinois Institute of Technology, Chicago, IL, USA.

ABSTRACT

Two new radar signal models using nonlinear frequency modulation are proposed and investigated with respect to enhancing the target's range estimation and reducing the sidelobe level. The performance of the proposed signal models is compared to the currently popular linear and nonlinear frequency modulation signal models. The Cramer Rao Lower Bound along with main lobe width and the peak to sidelobe ratio are used for comparing the signal models to show that better range accuracy and smaller sidelobes can be achieved with the proposed signal models.

Index Terms— frequency modulation, NLFM, matched filter, radar, CRLB, PSLR.

1. INTRODUCTION

Estimating the range and velocity of a moving target using radar has been investigated for a long time but is still an active research area. As targets get stealthier and harder to detect, accurate estimates of the target parameters are increasingly difficult to achieve. Options that can improve the accuracy of the parameter estimates are thus important.

One of the crucial radar system components that directly influences the accuracy of the target parameter estimates is the signal model itself. Models can be broadly classified into Frequency Modulation (FM) and Phase Modulation (PM). FM is more widely used because of its ease of generation and effective bandwidth usage; it will be the focus of this paper.

The FM signal model for radar has a long history of use and is discussed in detail in many texts [1, 2, 3, 4]. For example, the Linear Frequency Modulated signal (LFM, also known as chirp signal) introduced in 1940s remains the most frequently used signal model in radar systems. In LFM the signal's frequency is varied linearly with time across the signal's bandwidth. In this paper we generalize this signal model to a broader class in which the frequency is increased monotonically with time but not necessarily in linear form.

Generally the design of Nonlinear FM (NLFM) signals starts by specifying a desired power spectral density (PSD) (corresponding to the desired auto correlation (AC) function). Then applying the principle of stationary phase (sections 3.2

and 3.3 in [5]), a nonlinear frequency/phase function is obtained either by deriving the analytical solution or by using iterative numerical methods. Cook [6] used this principle to design NLFM signals which have PSDs with a raised cosine shape. This signal model exhibited smaller sidelobes when perfectly matched but resulted in higher sidelobes for even a moderate shift in the Doppler frequency. Usually the envelope of the signal is kept constant so that the power amplifiers in the transmitter can operate at their maximum efficiency. The hybrid-FM model, which has better Doppler tolerance, is discussed in [7], but the designed signal does not have a constant envelope thus resulting in SNR loss and widening of the AC main lobe in the receiver. Levanon and Mozeson discuss an empirically derived NLFM model (equation (5.20) in section 5.2 of [1], hereafter referred as NLFM-LM) which has good peak to sidelobe ratio (PSLR) performance. Many subsequent papers followed a similar strategy of starting from the required PSD and applying the constant envelope constraint to obtain the radar signal. For instance work in [8] analyzes many PSDs having the form of popular window functions and compares the PSLR and main lobe width, while [9] proposes a signal model that has similar instantaneous frequency characteristics resembling that of [6] but can achieve smaller sidelobe levels by extending the tail of the spectrum beyond the allowed bandwidth range. Many other PSDs have been proposed in [10] and [11] using the same design principle of [6] to obtain the phase function. A similar design method is used even when the available spectrum is not continuous [12, 13].

In this paper we present two parametrized NLFM signal models and assess the effect the parameters have on performance. The variance lower bound of the range estimate is inversely proportional to the second derivative of the ambiguity function (AF) (section 10.2.1, of [2]). With the signal buried in additive white Gaussian noise (AWGN), the variance lower bound is inversely proportional to the square of the first derivative of the signal (see section 3.1). The proper signal parameter choice can achieve larger first derivative thus reducing the variance lower bound on the range estimate.

In contrast to the range estimate (which depends on modulation type and bandwidth), the target's velocity estimate depends on the signal's duration (Chapter 10, Example 4 in [2]) and the carrier frequency (since larger carrier frequency results in larger Doppler shift). Yet the delay-Doppler coupling

of the AF can make the velocity and range errors correlated. AF analysis for the delay-Doppler coupling is not presented in this paper and is being carried out as a future work.

This paper is organized as follows. The signal models are discussed in section 2. We will concentrate only on the baseband version of the signal models as the frequency varies from 0 to B Hz. This can easily be generalized to the higher frequencies through modulation. Since our design approach focuses on reducing the lower bound of the range estimate, we present the comparison of Cramer Rao Lower Bound (CRLB) for various values of the nonlinearity parameter in section 3.1. Then we present the trade-off between achieving accurate range estimate (by reducing the AC main lobe width) versus achieving high PSLR in section 3.2. Simulation results presented in section 4 demonstrate the potential for improved performance with the new signal models. Finally we summarize our work in section 5.

2. SIGNAL MODELS

In the LFM signal model the frequency is linearly swept from 0 to B Hz. In this section we will consider a broader class of signals whose instantaneous frequency $f(t)$ monotonically increases from 0 to B Hz in a more general way as time goes from 0 to T seconds. The expression for the corresponding signal can be written as

$$s(t) = \sin(\phi(t)) \quad (1)$$

where

$$\phi(t) = 2\pi \int_0^t f(\lambda) d\lambda. \quad (2)$$

2.1. Signal Model 1: Time Exponentiated Frequency Modulation (TEFM)

One way to monotonically increase the frequency is through the following expression:

$$f(t) = B \left(\frac{t}{T} \right)^{\alpha-1}. \quad (3)$$

The corresponding signal expression obtained by substituting (3) in (1) and (2) is

$$s(t) = \sin \left(2\pi B \frac{t^\alpha}{\alpha T^{\alpha-1}} \right). \quad (4)$$

The parameter α controls the frequency evolution with respect to time. Choosing $\alpha = 2$ corresponds to the LFM. Figure 1 shows the frequency function $f(t)$ with respect to time for various values of α . It can be observed that for $\alpha = 2$, $f(t)$ reaches $B/2$ (50% of bandwidth) exactly at time $T/2$. When $1 < \alpha < 2$, $f(t)$ crosses $B/2$ earlier than $T/2$, spending more time in the higher frequencies. Since $f(t)$ varies slowly in this frequency region, its time derivative is smaller. According to

the stationary phase principle, this results in larger energy in the corresponding higher frequency region. For $\alpha > 2$, $f(t)$ spends more time in the lower frequencies (less than $B/2$) most of the time, emphasizing the lower frequencies.

Plots in the left column of Fig. 2 show the energy distribution for different values of α . One can observe that for $\alpha = 1.5$, the higher frequency region (around $B/2$ to B Hz) is emphasized and for $\alpha = 5$, the lower frequency region is emphasized ($< B/2$). For $\alpha = 2$, the energy is spread almost equally in the entire region. This matches with the prediction noted earlier. We will refer to this model as Time Exponentiated Frequency Modulation (TEFM) in the following sections.

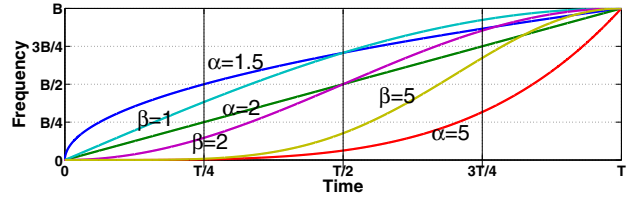


Fig. 1. Frequency vs Time of eqn (3), (5) for various α and β .

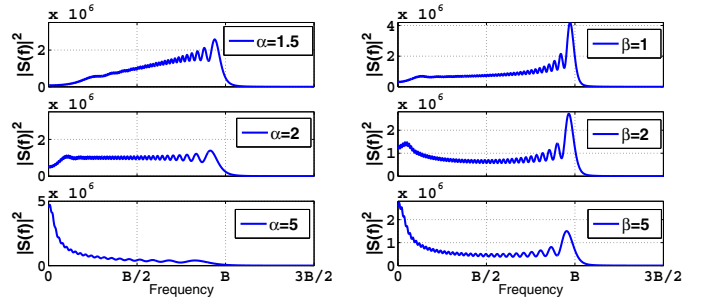


Fig. 2. Energy distribution for various α of (3), and β of (5).

2.2. Signal Model 2: Sine Exponentiated Frequency Modulation (SEFM)

One other way of changing the frequency with respect time is with a sinusoidal function. A general expression for the frequency as a function of time is

$$f(t) = B \sin^\beta \left(\frac{\pi t}{2T} \right). \quad (5)$$

The expression for the corresponding signal is

$$s(t) = \sin \left[2\pi B \int_0^t \sin^\beta \left(\frac{\pi \lambda}{2T} \right) d\lambda \right]. \quad (6)$$

In this case β controls the energy distribution in the frequency domain. For fractional values of β it is not possible to get the closed form expression and hence the phase has to be computed using numerical integration methods.

Also shown in Fig. 1 is the frequency evolution for this signal model for various values of β . For $0 < \beta < 2$, $f(t)$ spends more time on the higher side of $B/2$, emphasizing the higher frequencies. But the $\beta = 2$ curve spends more time in the very low and very high bandwidth regions compared to the mid-bandwidth region, emphasizing the flanks of the allowed bandwidth. Finally, $\beta > 2$ tend to concentrate more energy in the lower frequencies, by spending more time in that region.

This can be observed in the figures on the right column of Fig. 2. For $\beta = 1$, the emphasis is on the higher frequency side ($> B/2$) and for $\beta = 5$, the emphasis is on the lower frequency side ($< B/2$). But for $\beta = 2$, energy is spread almost evenly over the middle part of the frequency region with more emphasis on the lower and higher side of the bandwidth. We will refer this model as Sine Exponentiated Frequency Modulation (SEFM).

3. PERFORMANCE COMPARISON OF THE SIGNAL MODELS

Here we assess the impact of α and β on the signal models' ability for accurate range estimation and smaller sidelobes using the CRLB and the shape of AC. We compare the performance to LFM and NLFM-LM of [1] (with $B_L = 2B$ and $B_C = 0.1B$, where B is the given bandwidth). The parameters of NLFM-LM are chosen such that the bandwidth is comparable with that of the proposed signal models.

3.1. Variance of Range Estimation

Local accuracy of the target parameters is analyzed by relating the Fisher Information Matrix (FIM) to the AF in section 10.2.1 of [2]. Hence FIM can be used for choosing α and β for which the CRLB is small. In this section we derive the FIM with respect to round trip delay time and Doppler frequency for the proposed signal models. Since the resulting FIM is ill-conditioned, the reciprocal of the corresponding diagonal elements of FIM is used for CRLB [14, 15]. To do this we compute the CRLB for both the proposed signal models in AWGN for various α and β . Since we are just interested in the relative CRLB, we normalize with the CRLB of LFM (TEFM with $\alpha = 2$).

If $s(t) = \sin(\phi(t) + 2\pi f_c t)$, $0 \leq t \leq T$, is the transmitted signal, the reflected signal is of the form

$$r_s(t) = \sin(\phi(t - \tau) + 2\pi(f_c + f_d)(t - \tau)), \quad (7)$$

where $\phi(t)$ is the phase of the signal defined in equations (4) and (6). f_c is the carrier frequency and f_d is the Doppler frequency shift caused by the moving target. The parameter τ is called the round trip delay time and depends on the target range (R) as $\tau = \frac{2R}{c}$. The transmitted signal pulse duration is T and the total time is $T_o = T + \tau_{max}$ where τ_{max} is the maximum time delay.

The discrete version of the received signal is

$$r(n; n_0) = \begin{cases} w(n) & 0 \leq n < n_0 \\ r_s(n; n_0) + w(n) & n_0 \leq n < n_0 + M \\ w(n) & n_0 + M \leq n \leq L - 1 \end{cases}$$

where $w(n)$ is assumed to be AWGN with variance σ^2 , $r_s(n; n_0) = \sin(\phi(n\Delta - n_0\Delta) + 2\pi(f_c + f_d)(n - n_0)\Delta)$, Δ is the sampling interval and $n_0 = \tau/\Delta$, $M = T/\Delta$, $L = T_o/\Delta$. With this formulation, the CRLB of n_0 (discrete time version of τ) is (section 3.5 in [16])

$$var(\hat{n}_0) \geq \frac{\sigma^2}{\sum_{n=0}^{L-1} \left(\frac{\partial r_s(n; n_0)}{\partial n_0} \right)^2}. \quad (8)$$

For TEFM, the variance lower bound can be shown to be

$$var(\hat{n}_0) \geq \frac{\sigma^2}{(2\pi B\Delta)^2 \sum_{n=0}^{M-1} \left(\frac{n\Delta}{T} \right)^{2(\alpha-1)} \cos^2(\phi_r(n\Delta))} \quad (9)$$

and for SEFM the lower bound is given by

$$var(\hat{n}_0) \geq \frac{\sigma^2}{(2\pi B\Delta)^2 \sum_{n=0}^{M-1} \sin^{2\beta} \left(\frac{\pi n\Delta}{2T} \right) \cos^2(\phi_r(n\Delta))} \quad (10)$$

where $\phi_r(n\Delta) = \phi(n\Delta) + 2\pi(f_c + f_d)(n - n_0)\Delta$ and $\phi(t)$ is given by the phase arguments in (4) and (6). Figure 3 shows the CRLB as a function of α and β for both the signal models.

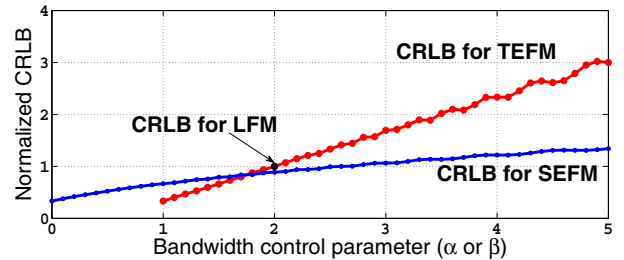


Fig. 3. CRLB comparison for both the signal models.

One can observe that the CRLB increases generally with α and β . Hence having smaller α and β improves performance by reducing the variance lower bound of the τ estimate (and hence the target's range estimate). On other hand, CRLB for the Doppler estimate for both the signal models is

$$var(\hat{f}_d) \geq \frac{\sigma^2}{(2\pi\Delta)^2 \sum_{n=0}^{M-1} n^2 \cos^2(\phi_r(n\Delta))}. \quad (11)$$

In this case, the nonlinearity parameters α or β affect the summation only via the phase term which is approximately $\frac{1}{2} \sum_{n=0}^{M-1} n^2$. Hence the variance lower bound for Doppler is not affected by the signal model.

For TEFM, the minimum value for α is 1. In this case, the entire signal energy is concentrated at a single frequency B

Hz. Though this produces the lowest variance bound for the range estimate, this may not be an ideal choice. For example transmitting a sinusoid with high energy can easily expose the radar’s location to the adversary. Also the matched filter will have large sidelobes. Similar behavior can be expected for SEFM, as β is set to its minimum value 0.

3.2. Autocorrelation for Matched Filter

The most commonly used target parameter estimator in radar system is the matched filter (MF). In MF the reflected signal is correlated with the transmitted signal and the round trip delay time (τ) is given by the peak of the correlation function. Hence it is useful comparing the correlation function of these signal models to observe the main lobe width and the sidelobe levels. A narrow main lobe in the AC can be associated with an accurate range estimate of the target. It also helps in resolving two closely placed targets. Furthermore it is desirable to have smaller sidelobes. Otherwise the sidelobes from a larger target can mask the main lobe of a smaller target.

The AC is defined as

$$R(\nu) = \int_{-T}^T s(t) s^*(t + \nu) dt. \quad (12)$$

We show the comparison of the 3-dB main lobe width for the both signal models for various values of the nonlinearity parameters α and β in Fig. 4. The main lobe (ML) widths are normalized with respect to the LFM’s ML width (marked with black dot in the figure) for easy comparison. For TEFM mod-

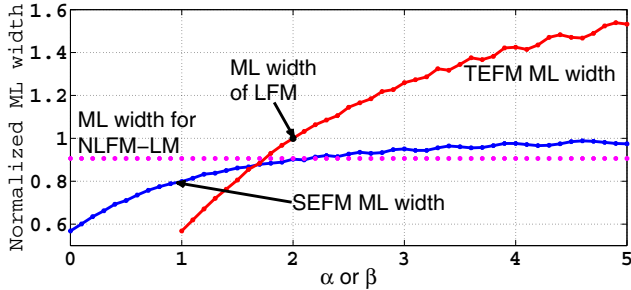


Fig. 4. 3-dB Normalized Main-lobe width.

els, the ML width is smaller compared to LFM for $1 < \alpha < 2$ and increases for $\alpha > 2$. This matches with what we observed with CRLB. We can also observe that ML width of TEFM is less than that of NLFM-LM for $\alpha < 1.8$. In CRLB plot we observe that for SEFM, variance lower bound on range estimate becomes worse than that of LFM beyond $\beta > 2.5$. But with matched filter estimator, AC is more resilient for SEFM and the ML width approaches to LFM’s only when $\beta > 4$. Also we can observe that the ML width of SEFM is less than that of NLFM-LM for $\beta < 2.3$.

The next important parameter of the AC is the PSLR, which gives a measure of sidelobe level with respect to main

lobe level. It is defined as

$$PSLR = \left| \frac{R(0)}{\max(R(\tau))} \right|, \quad 0 < \tau < T. \quad (13)$$

In Fig. 5, we plot the normalized PSLR (with respect to LFM’s PSLR) for both the signal models for various values of α and β . As can be observed, for $1 < \alpha < 2$ in TEFM, the PSLR values are small compared to LFM, meaning that sidelobes are larger compared to LFM. As $\alpha > 2$, the PSLR values become higher (indicating smaller sidelobes) and reach their maximum around $\alpha = 2.6$. Even after $\alpha = 2.6$ though sidelobe levels increase, they are still smaller than that of LFM. Also TEFM is able to achieve higher PSLR (smaller sidelobes) compared to NLFM-LM for $\alpha > 2$. SEFM achieves higher PSLR than LFM for $\beta > 1.6$ and compared to NLFM-LM, SEFM achieves higher PSLR for $\beta > 1.8$.

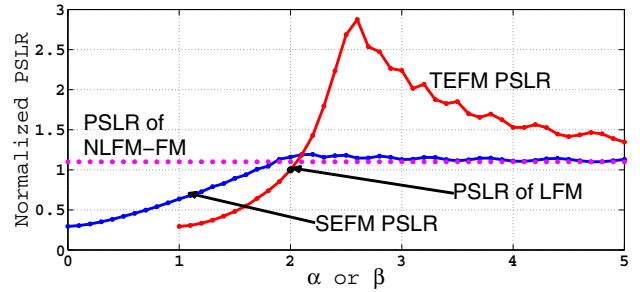


Fig. 5. Normalized PSLR.

In summary, with respect to LFM, TEFM model can have either narrower ML for $\alpha < 2$ or smaller sidelobes for $\alpha > 2$. But SEFM achieves narrower ML for $0 < \beta < 4$ and also can achieve smaller sidelobes for $\beta > 1.6$ compared to LFM.

3.3. Inference from the comparison metrics

For SEFM the reasonable operating region is between $1.6 < \beta < 2.5$ where the signal model achieves smaller variance and higher PSLR compared to LFM. Beyond this interval, the CRLB gets bigger than that of LFM and for $\beta > 4$ the peak sidelobe level for SEFM gets closer to that of LFM. But with TEFM signal model the designer has to choose between smaller ML width on the range estimate for $1 < \alpha < 2$ and higher PSLR for $\alpha > 2$. Though it may seem like a weakness for TEFM, for the applications where higher PSLR is required (such as dense targets scenario), TEFM with α around 2.6 would be a superior choice.

4. SIMULATION RESULTS

In this section we present the variance of target’s range computed from Monte Carlo simulation. For the simulation a target is assumed to be at the range of 100 km. The reflected

signal is modeled as given in eqn (7). The target range is computed from the round trip delay time of the reflected signal. The round trip delay is given by the delay corresponding to the maximum of the AC main lobe. Monte-carlo simulation is carried out for 1000 iterations for various SNR values with the signal parameters of bandwidth $B = 2 \times 10^6$ Hz and the signal time duration of $T = 10 \times 10^{-6}$ seconds. The variance of the range estimate computed from the simulations using the different signal models for a range of SNR values is presented in Table 1.

Table 1. Variance of range estimate

SNR (in dB)	LFM Var	TEFM($\alpha = 1.5$) Var	SEFM($\beta = 1.7$) Var
0	0.0058	0.0026	0.0042
-2.0	0.0080	0.0047	0.0070
-4.0	0.0118	0.0073	0.0096
-6.0	0.0166	0.0111	0.0133
-8.0	0.0277	0.0175	0.0214
-10.0	0.0418	0.0237	0.0307
-12.0	0.0663	0.0402	0.0497
-14.0	0.1054	0.0583	0.0661
-16.0	0.1636	0.0897	0.0927
-18.0	0.2690	0.1507	0.1795

We can observe that as the SNR decreases, the variance of the range estimate increases. However in all cases the LFM has larger variance compared to the other two cases. The order of the variance is as follows.

$$\text{Var}(LFM) > \text{Var}(\beta = 1.7) > \text{Var}(\alpha = 1.5). \quad (14)$$

This agrees with our deduction from section 3 that a small ML width make the range estimate accurate.

5. CONCLUSION

In this paper we have proposed general form for two nonlinear signal models (TEFM and SEFM). We analyzed energy distribution in the frequency domain. Then we presented the CRLB and PSLR performance for both the signal models. From the performance metrics we observed that the TEFM achieves smaller range variance for $1 < \alpha < 2$ and larger PSLR for $\alpha > 2$. And SEFM achieves both smaller range variance and higher PSLR for $1.6 < \beta < 2.5$. Finally we confirmed through Monte Carlo simulation that smaller range variance can be attained by proper selection of α and β for both the signal models.

6. REFERENCES

[1] N. Levanon and E. Mozeson, *Radar Signals*, Wiley-IEEE Press, 2004.

[2] H.L. Van Trees, *Detection, Estimation, and Modulation Theory, Part III: Radar-Sonar Processing and Gaussian Signals in Noise*, John Wiley & Sons, Inc., 2001.

[3] M.I. Skolnik, *Introduction to Radar Systems*, McGraw Hill, 2003.

[4] F.E. Nathanson, J.P. Reilly, and M.N. Cohen, *Radar Design Principles: Signal Processing and the Environment*, SciTech Publishing, Inc., 2006.

[5] C.E. Cook and M. Bernfeld, *Radar Signals: an Introduction to Theory and Application*, Academic Press, 1967.

[6] C.E. Cook, "A class of nonlinear fm pulse compression signals," *Proc. IEEE*, vol. 52, pp. 1369–1371, 1964.

[7] J. A. Johnston and A.C. Fairhead, "Waveform design and doppler sensitivity analysis for nonlinear fm chirp pulses," *IEE Proc. F*, vol. 133, pp. 163–175, 1986.

[8] Pan Yichun, Peng Shirui, Yang Kefeng, and Dong Wenfeng, "Optimization design of nlfm signal and its pulse compression simulation," in *Proc. IEEE Radar Conf.*, May 2005, pp. 383–386.

[9] C Leśnik, "Nonlinear frequency modulated signal design," *Acta Phys. Pol. A*, vol. 116, pp. 351–354, 2009.

[10] S. Boukeffa, Y. Jiang, and T. Jiang, "Sidelobe reduction with nonlinear frequency modulated waveforms," in *Proc. 7th Int. Colloq. Signal Process. and its Applicat.*, 2011, pp. 399–403.

[11] M. Zych, "Suppression of gpr range sidelobes based on nlfm signal," in *Proc. 13th Int. Radar Symp.*, 2012, pp. 454–458.

[12] L. Jackson, S. Kay, and N. Vankayalapati, "Iterative method for nonlinear fm synthesis of radar signals," *IEEE Trans. Aerosp. Electron. Syst.*, vol. 46, pp. 910–917, April 2010.

[13] L.K. Patton, C.A. Bryant, and B. Himed, "Radar-centric design of waveforms with disjoint spectral support," in *Proc. IEEE Radar Conf.*, May 2012, pp. 269–274.

[14] B. Z. Bobrovsky, E. Mayer-Wolf, and M. Zakai, "Some classes of global cramer-rao bounds," *Ann. Stat.*, vol. 15, no. 4, pp. 1421–1438, 1987.

[15] A.A. Nasir, H. Mehrpouyan, and R.A. Kennedy, "New expression for the functional transformation of the vector cramer-rao lower bound," in *Proc. 14th IEEE Workshop Signal Process. Advances Wireless Commun.*, June 2013, pp. 395–399.

[16] Steven M. Kay, *Fundamentals of Statistical Signal Processing: Estimation Theory*, Prentice-Hall, Inc., 1993.